Calorimetric study of magnetic fluids under a magnetic field

Susamu Taketomi* and Christopher M. Sorensen
Department of Physics, Kansas State University, Manhattan, Kansas 66506, USA

Kenneth J. Klabunde
Department of Chemistry, Kansas State University, Manhattan, Kansas 66506, USA

(Received 1 July 2002; published 1 August 2003)

In our past study, it was found that the strong magneto-optical effect of a magnetic fluid (MF) under a magnetic field is due to the second-order phase transition from colloidal particles' monodispersed phase to the particles' anisotropically agglomerated microclusters phase. These results, however, contradicted the Landau criterion. In the present study, in order to clarify whether the transition is of first order or second order, we performed differential scanning calorimetry (DSC) experiments on three different MFs to look for the existence of a phase transition latent heat. The DSC measurement was performed in the temperature range 22–150 °C with zero magnetic field and under ≈10 kA/m magnetic field, respectively. No phase transition heat was observed within an experimental error of 0.03 kJ/kg for all the samples whether or not the field was applied.

DOI: 10.1103/PhysRevE.68.021501 PACS number(s): 64.70.Ja, 75.30.−m, 75.40.−s, 75.50.Mm

I. INTRODUCTION

A. Interaction between colloidal particles in magnetic fluid and cluster formation

A magnetic fluid (MF) is a colloidal solution containing ferromagnetic or ferrimagnetic colloidal particles stably dispersed in a solvent with special surface active agents or surfactants [1,2]. Conventionally, it has been believed that the individual magnetic colloidal particles are monodispersed in the solvent, the interaction between the particles is negligible; and, accordingly, each particle's permanent magnetic moment rotates freely in the solvents and macroscopically the MFs show a typical superparamagnetic behavior. But the MFs' several contradictory experimental results under magnetic fields, such as their strong magneto-optical effects [3], anisotropic propagation of sound [4], and spin-glass-like behavior of the complex magnetic susceptibility [5], indicated an interaction between the colloidal particles or an instantaneous generation of anisotropic agglomerates of the colloidal particles under the magnetic field. Under an external magnetic field, the interaction between the colloidal particles induces coupling of particles, which forms clusters which, however, instantaneously break up due to the weakness of interaction. In fact, some MFs of less dispersivity of the colloidal particles show needlelike clusters of micron size scale generation under the magnetic field, as observed by an optical microscope [6], and the clusters' various properties were studied [7–9]. Recently, Donselaar *et al.* revealed that even under no field there exist the colloids' clusters of submicron scale [10]. Quenching the MFs they obtained a frozen MF thin film. They observed this frozen film with an electron microscope and found these clusters. It is consistent with the experimental fact that there is a weak birefringence even under no magnetic field [11,12]. A recent discovery of the difference in normalized initial magnetic susceptibility of the MFs and their highly diluted solution also supports the above speculation [13]. Here, the normalized initial magnetic susceptibility is the initial susceptibility divided by the colloid volume fraction. Cluster formation, even with zero field, causes a difference in the normalized initial magnetic susceptibility between the mother MF and its highly diluted solution. This cluster formation under the external field is the origin of the peculiar macroscopic law of the magnetic fluid's magnetic birefringence, which is described in the next paragraph.

The typical phenomenon caused by cluster formation of the colloidal particles in the MFs is magnetic birefringence.

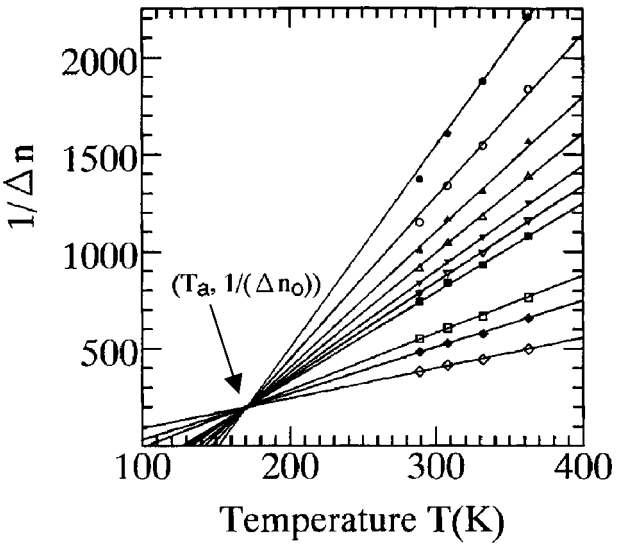

FIG. 1. Temperature dependence of magnetic fluid's birefringence under several constant fields. Marks in the figure denote the following constant fields strength: ●, $H=31.8$ kA/m; ○, $H=39.8$ kA/m; ▲, $H=47.7$ kA/m; △, $H=55.7$ kA/m; ▼, $H=63.7$ kA/m; ▽, $H=71.6$ kA/m; ■, $H=79.6$ kA/m; □, $H=159$ kA/m; ◆, $H=239$ kA/m; and ◇, $H=637$ kA/m. The magnetic fluid was two-times diluted FV-42.

*Present Address: Nat'l. Inst. Stand. Tech., Gaithersburg, MD 20899-8552. Permanent address: Matsumoto Yushi-Seiyaku Co. Ltd., Yao, Osaka 581-0075, Japan. FAX: 1-301-975-4553; Corresponding author. Email address: taketomi@nist.gov

We have already found a peculiar temperature dependence of the birefringence Δn [14–17]. Figure 1 is one such example [17]. The inverse of the birefringence is a linear function of temperature T under a constant external magnetic field H. In addition, lines corresponding to constant field intersect at one point on a $(1/\Delta n)-T$ graph. This relation is expressed by

$$\Delta n = \frac{\Delta n_o f(H)}{\frac{T}{T_a} - 1 + f(H)}, \tag{1}$$

where T_a and Δn_o are positive constants denoting the coordinates of the crossing point of lines in Fig. 1, and the function $f(H)$ is an increasing function of H. The term $T_a[1-f(H)]$ corresponds to the Curie temperature T_C of the Curie-Weiss law. Hereafter in this paper, we will refer to Eq. (1) as the generalized Curie-Weiss law. This peculiar law was experimentally confirmed by other researchers [18,19].

B. Colloidal particles' cluster formation as phase transition of second order

The colloidal particles in the MFs coagulate under an external magnetic field and make clusters of elongated shape in the field direction. This formation of anisotropic clusters is the origin of magnetic dichroisms and the magnetic birefringence of the MFs.[1] The formation of these clusters, however, instantaneous and the clusters decompose in the next moment as generation and annihilation of bubbles in boiling water. Accordingly, the generation and annihilation of the clusters in the MF correspond to a certain critical state. In fact, there exist several scaling relations among the physical variables related to the MF properties [14–16]. Now we consider the change from the colloidal particles' monodispersed state to the state in which the clusters are formed, as phase transition, and an order parameter Δ is introduced as follows. For convenience, let all the colloid particles be assumed to be spheres of the same radius. The clusters' averaged electric depolarization factor $\langle N\rangle$ in the magnetic field direction is expressed by [14]

$$\langle N\rangle = \frac{1}{\phi}\sum_{k=1}^{\infty} k v_o \nu_k N_k . \tag{2}$$

Here, ϕ is the volume fraction of the colloidal particles, v_o is the volume of each particle, and ν_k is the number of clusters consisting of k colloidal particles per unit volume of the MF, where we also assumed that the clusters consisting of the k colloidal particles have the same shape. Then, the birefringence Δn is expressed by

$$\Delta n = (\Delta n_{\mathrm{sat}})(1-3\langle N\rangle), \tag{3}$$

where Δn_{sat} is a positive constant [14,16]. If an order parameter Δ, defined as

$$\Delta \equiv 1-3\langle N\rangle, \tag{4}$$

is introduced, Eq. (3) is rewritten as

$$\Delta n = (\Delta n_{\mathrm{sat}})\Delta, \tag{5}$$

i.e., the birefringence Δn is proportional to the order parameter Δ.

The MF's free energy G is expressed using the Landau formalism by

$$G(T,H,\Delta) = G_o(T,H) + \frac{a}{2}\left(\frac{T}{T_a} - 1 + f(H)\right)\Delta^2 + \epsilon\Delta^3 + b\Delta^4 - \gamma f(H)\Delta, \tag{6}$$

where a, b, γ, and ϵ are constants possessing the same dimension of $G(T,H,\Delta)$ (J/m^3) and $G_o(T,H)$ is the free energy of the magnetic fluid with $\Delta=0$ or without agglomeration [16,17]. (a, b, and γ are positive.) We neglect other variables such as pressure in this paper because they are irrelevant to the present subject. We assumed the phase transition with respect to Δ to be of second order; accordingly,

$$\epsilon = 0 \tag{7}$$

was assumed [14,16,17]. From the equilibrium condition,

$$\frac{\partial G(T,H,\Delta)}{\partial \Delta} = 0, \tag{8}$$

we obtain

$$\Delta = \frac{\gamma}{a}\cdot\frac{f(H)}{\frac{T}{T_a} - 1 + f(H)}. \tag{9}$$

Now Eq. (9) is equivalent to Eq. (1) from Eq. (5). Consequently, the peculiar law of MF's magnetic birefringence, or the generalized Curie-Weiss law, is obtained from Landau's phase transition theory of second order.

After some similar research, we found that almost all the clusters in the magnetic fluids under the field had a needlelike shape. Accordingly, N_k in Eq. (2) should be 0, except for $k=1$. Consequently, Eq. (2) is simply expressed by

$$\langle N\rangle = \frac{1}{3}\frac{\phi_{\mathrm{mon}}}{\phi}, \tag{10}$$

where ϕ_{mon} is the volume fraction of the colloidal particles which are monodispersed in the MF. Note that Eq. (10) is obtained without artificial assumptions, such as all the colloidal particles are spheres of the same radius. Let ϕ_{agg} de-

[1] If the MF is highly diluted, the cluster formation of the colloidal particles no longer occurs due to the weakening of the mutual interaction between the colloidal particles. It still shows a very weak birefringence under the magnetic field [20,21]. It is, however, not due to the elongated cluster formation but due to the shape anisotropy of the colloidal particles. This kind of weak magnetic birefringence was known as the Majorana effect a long time ago [22]. It is, however, different from what we are discussing in the present paper.

note the volume fraction of the colloidal particles which aggregate, and using the relation

$$\phi_{\mathrm{agg}}+\phi_{\mathrm{mon}}=\phi, \tag{11}$$

Eq. (4) is expressed by

$$\Delta=\frac{\phi_{\mathrm{agg}}}{\phi}. \tag{12}$$

Accordingly, the order parameter Δ denotes the fraction of the aggregated particles over all the particles. This theory interpreted not only the MF's magnetic birefringence but also its magnetic dichroism correctly [14,23].

There was a strong objection against the above argument. According to the Landau theory, the transition of the anisotropic cluster formation cannot be a transition of second order [24]. As a matter of fact, the isotropic-nematic transition of the liquid crystal of rodlike molecules is a transition of first order [25]. Therefore, the coefficient ϵ of the third-order term in Eq. (6) should not be 0 and, consequently, Eq. (9) cannot be derived. In 1970s, however, Alexander and Amit proved that even in such a case, the transition can be of second order [26]. They showed that if the energy barrier between the neighboring energy minima is small, the phase transition of first order changes to the transition of second order if fluctuations are taken into account.

Consequently, we have to conduct concrete experiment to determine whether or not this phase transition is of second order. The most suitable experiment for this determination is a calorimetric experiment. If the transition is of first order, there should be heat discharge or absorption accompanying the transition. We can determine whether or not it is a second-order transition by measuring the heat discharge or absorption.

II. EXPERIMENTAL METHODS

A. Principle of differential scanning calorimeter

Differential scanning calorimeter (DSC) is suitable for the MF's calorimetric measurement because it is not necessary to leave the sample in a vacuum chamber to get the precise measurement [27]. We performed the MFs' calorimetric measurement from the room temperature up to 150 °C with zero field and under an applied magnetic field. We left a permanent magnet fragment together with the MF in the sample holder so that the MF is under a magnetic field. Accordingly, the MF was not under a uniform magnetic field when the calorimetric measurement was made. However, the primary purpose of the present experiment was to determine if there was heat discharge or absorption accompanying the phase transformation under the magnetic field. Neither the precise phase transition temperature nor the precise heat measurement for the phase transition was necessary for the present experiment. Accordingly, the field's nonuniformity was irrelevant for the present experiment. A schematic structure of the DSC experiment under a magnetic field is shown in Figs. 2(a) and 2(b). However, when the DSC measurement was made with zero magnetic field, no magnet fragment existed

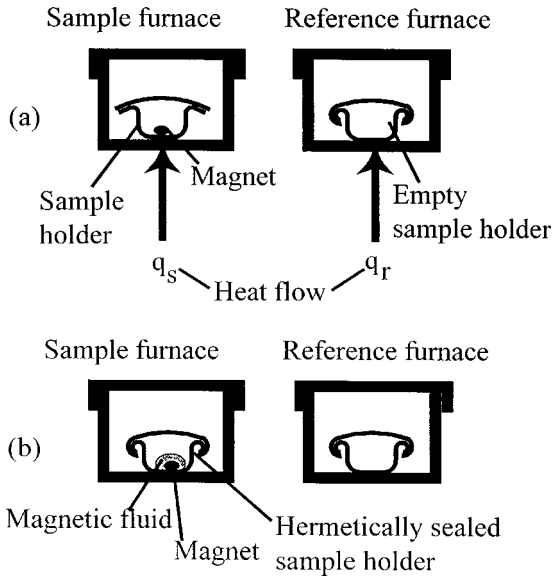

FIG. 2. DSC measurement principle under a magnetic field (a) base line measurement and (b) DSC measurement of MF. The magnetic field was applied by a magnet fragment.

in Figs. 2(a) and 2(b). A sample holder with a sample is left in a sample furnace and a similar sample holder alone is left in a reference furnace. The sample furnace and the reference furnace were similar and they were adiabatically isolated from each other. Heat flows q_s (J/sec) and q_r (J/sec), which flowed to the sample furnace and the reference furnace, respectively, from the electric heaters were controlled so that both furnace temperatures were equal and rose at the same constant rate β (K/sec). The measured physical quantity was the heat flow difference $q\equiv q_s-q_r$ at temperature T (K). The relation between q and the sample's specific heat c [J/(kg K)] is expressed by [28]

$$q=\beta mc, \tag{13}$$

where m is the sample mass (kg). If the q-T graph has an upward or a downward peak, it shows endothermic or exothermic heat, respectively, and the heat amount is obtained from the peak area. In the real experiment, there is a heat flow difference even if there is no sample due to the difference between the two furnaces in heat leakage, furnace structure, and sample holder.

For the zero magnetic field measurement, we performed the experiment as follows. We first measured the background heat flow difference q_{bg} when the sample did not exist [Fig. 2(a) without a magnet fragment]. Then we measured the heat flow difference q_{ex} when the sample holder was filled with the sample [Fig. 2(b) without a magnet fragment]. Finally, the real heat flow difference q was obtained by

$$q\equiv q_{\mathrm{ex}}-q_{\mathrm{bg}}. \tag{14}$$

A differential scanning calorimeter, Pyris I, purchased from the Perkin Elmer Co. was used for the present experiment. The sample holder consisted of an aluminum pan and lid which were also purchased from the Perkin Elmer. The pan

TABLE I. Characteristics of samples. Saturation magnetization is, for convenience, the magnetization at $H=716$ kA/m.

Sample	A_1	A_2	B_1	B_2	C_1	C_2
Commercial name of MF	FW-40	FW-40	FNC-50	FNC-50	FV-42	FV-42
Colloidal particle	Magnetite	Magnetite	MnZn ferrite	MnZn ferrite	Magnetite	Magnetite
Solvent	Water	Water	Paraffine oil	Paraffine oil	Alkylnaphthalene	Alkylnaphthalene
Specific gravity (kg/m^3)	1.37×10^3	1.37×10^3	1.35×10^3	1.35×10^3	1.36×10^3	1.36×10^3
Colloid volume fraction	0.091	0.091	0.125	0.125	0.104	0.104
Saturation magneterization (kA/m)	35.3	35.3	36.4	36.4	26.4	26.4
MF mass (mg)	12.4	16.4	9.4	9.2	11.9	12.6
Magnet mass (mg)		4.6		3.0		11.1
Max field (kA/m)		19		16		18
Average field (kA/m)		9.5		8.0		8.0

was 4 mm in diameter and 2 mm in depth. After putting the MF in the pan, the lid was covered on the pan and they were hermetically sealed by a press machine.

The measurement under a magnetic field was performed as follows. First, we measured the background heat flow difference q_{bg} when the permanent magnet fragment alone existed in the sample holder of the sample furnace [Fig. 2(a)]. Then filling the sample holder with MF together with the permanent magnet fragment followed by hermetical sealing, we measured q_{ex} [Fig. 2(b)]. By subtracting q_{bg} from q_{ex}, we removed the magnet's calorimetric contribution and accordingly $q\equiv q_{\mathrm{ex}}-q_{\mathrm{bg}}$ contained the MF's calorimetric contribution alone.

We used magnetized samarium cobalt as the permanent magnet. For each experiment, a different magnet fragment was used. The size of the fragments was a few millimeter and their weight was tabulated in Table I. Before the experiment, we removed the magnet's thermal demagnetization effect by exposing it under heat cycles several times between room temperature and 200 °C. After this treatment, no further thermal demagnetization was observed. The magnetic field strength was estimated by measuring the field strength on the magnet surface with a Hall probe magnetometer. The maximum and average magnetic field H on the magnet surface were tabulated in Table I. In the present paper, we use SI units and the magnetization $\boldsymbol{M}$ is defined by $\boldsymbol{B}=\mu_o(\boldsymbol{H}+\boldsymbol{M})$, where $\boldsymbol{B}$ is the magnetic flux density and $\mu_o=4\pi\times10^{-7}$ H/m is the magnetic permeability in vacuum.

Instead of spreading on the bottom of the sample holder, the MF was attracted to the magnet fragment and covered its surface. Accordingly, it is conceivable that the field strength that the MF experienced was distributed in the considerably narrow region. The change of the magnetic field strength or field distribution by adding the MF was negligible. The ordinary MF's saturation magnetization M_{sat} is of the order of 40 kA/m, while the present permanent magnet's residual magnetization M_r was of the order of 600 kA/m. Accordingly, the introduction of the MF into the sample holder did not make a significant difference in the magnetic field strength distribution in the sample furnace region. Therefore, Eq. (14) holds to a good approximation in the present experiment.

B. MF samples

Three different MFs: Marpomagna FW-40, FNC-50, and FV-42 prepared by Matsumoto Yushi-Seiyaku Co. were used. We have already made an optical microscope observation and the visible light scattering experiment of these MFs [29]. MF FN-50 in Ref. [29] is the same as MF FNC-50 of the present paper. MF FW-40 is a magnetite colloidal particle, water solvent MF in which the clusters were most easily formed under the magnetic field amongst the three MFs. We observed by the optical microscope that macroclusters were formed under the field as weak as 1 kA/m at room temperature. Here, the macrocluster is a cluster of the colloidal particles, the scale of which amounts to as large as a few micrometers and which can be easily observed by the optical microscope. On the other hand, we denote the cluster, the scale of which is less than a submicron order and which cannot be observed by the optical microscope, as a microcluster. MF FNC-50 was MnZn ferrite colloidal particle, paraffin oil solvent MF in which the macroclusters were generated under a magnetic field as weak as 10 kA/m at room temperature. The clusters disappeared at temperatures as low as 60 °C. MF FV-42 is magnetite colloidal particle, alkylnaphthalene solvent MF, in which no macroclusters were generated under a field as high as 100 kA/m. This MF is the most stable MF among the three MFs. It, however, shows birefringence under the field. Accordingly, it is conceivable that the microclusters are formed in MF FV-42 in the presence of the field.

Samples A_1 and A_2 contained the MF FW-40. In the same manner, samples B_1 and B_2 and samples C_1 and C_2 contained the MFs, FNC-50 and FV-42, respectively. Samples A_1, B_1, and C_1 were used for the DSC measurement with zero field. Samples A_2, B_2, and C_2, which contained magnet fragments, were used for the DSC measurement under a magnetic field. The sample characteristics are tabulated in Table I.

III. EXPERIMENTAL RESULTS

The samples B_1, B_2, C_1, and C_2 were measured at temperatures from 22 °C up to temperatures as high as 150 °C, while the samples A_1 and A_2 were measured at temperatures from 22 °C up to temperatures as high as 95 °C due the water

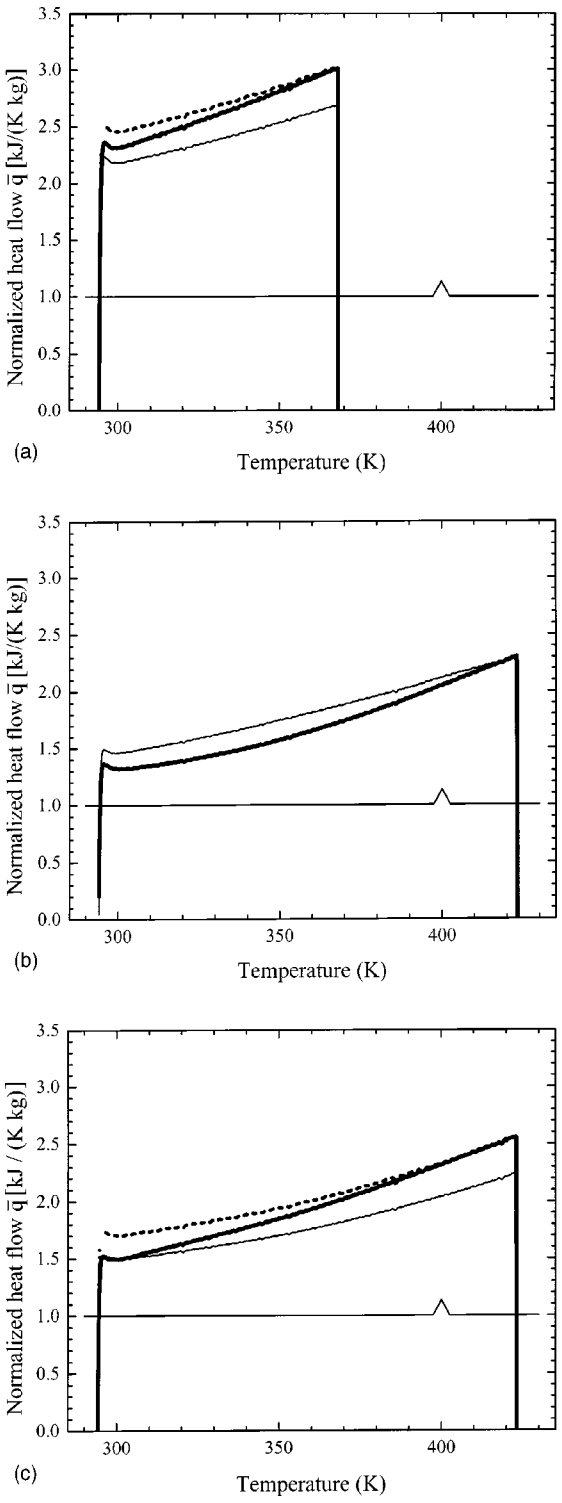

FIG. 3. Normalized heat flow $\overline{q}$ as a function of temperature T (a) samples A_1 and A_2 or MF FW-40, (b) samples B_1 and B_2 or MF FNC-50, and (c) samples C_1 and C_2 or MF FV-42. Thin solid lines denote with zero magnetic field and thick solid lines denote under a magnetic field. Broken lines denote renormalized $\overline{q}$-T curves with zero field so that the renormalized $\overline{q}$ coincide with $\overline{q}$ under the field at the maximum experimental temperature. Horizontal line with a small triangle peak is a virtual line to compare the peak area. The triangle peak area is 334 J/kg which is 1/1000 of the latent heat of water from liquid to ice.

solvent. The temperature rise rate β was 1/30 °C/sec for all the measurements.

Figures 3(a)–3(c) show the experimental results of the samples A_i, B_i, and C_i, respectively [$i=1$ (no magnetic field) and 2 (under a magnetic field)]. The normalized heat flow $\overline{q}$ is shown as a function of temperature T in each figure. Here, the normalized heat flow $\overline{q}$ is defined by

$$\overline{q} \equiv \frac{q}{\beta m}. \tag{15}$$

From Eq. (13), if there is no heat discharge or absorption, the normalized heat flow $\overline{q}$ is equivalent to the specific heat. If there is a peak in the $\overline{q}$-T curve, the peak area is the heat discharge or absorption per unit mass of the sample. Thin solid lines in Figs. 3(a)–3(c) denote $\overline{q}$ as a function of temperature T with zero field, while thick solid lines denote the $\overline{q}$-T curves under a magnetic field or with the magnet fragment. The small peaks around $T=22$ °C were due to overshoots accompanying the beginning of the temperature rise, and they did not imply the heat absorption.

The MF phase at room temperature under the field is the phase having clusters. The existing clusters decomposed with the temperature rise and the MF phase changed to colloid-monodispersed phase. If this phase transition is of first order, a peak of the heat discharge or absorption should appear in the $\overline{q}$-T curve. The peak should be rather broad due to the nonuniformity of the magnetic field. Even if we take this broadening into account, the experimental results, however, showed no peaks in Figs. 3(a)–3(c). The fluctuation of the $\overline{q}$-T curves is due to the fluctuation in the controlled temperature. For convenience, virtual triangular peaks are shown in Figs. 3(a)–3(c). The triangle area is 0.334 kJ/kg, which is equivalent to 1/1000 of water latent heat from solid to liquid. The fluctuation area due to temperature fluctuation is ≈0.03 kJ/kg. Accordingly, it is concluded that the present transition is not a first-order transition with the experimental precision of 0.03 kJ/kg.

In Fig. 3(b), the normalized $\overline{q}$ of sample B_2 or under the magnetic field was less than that of B_1 or with zero field in the all-temperature region. In addition, they are almost equal at the maximum temperature. An opposite relation was obtained for sample couples A_1-A_2 in Fig. 3(a) and C_1-C_2 in Fig. 3(c). These experimental relations were, however, not significant. The MF sample quantity was so small (about 10 mg in order of magnitude) that the effective digit of the sample mass was only 2 in measurement. In addition, as the MF was liquid, some amount of solvent in the MF evaporated before the sample holder was hermetically sealed. In the present experiment, we sealed the sample holder as soon as the MF mass in the holder pan was measured. But the evaporating mass ratio might not be negligible due to the smallness of the MF's mass itself. A considerable experimental error in the absolute value of $\overline{q}$ is caused by the uncertainty of m. In addition, the thermal contact between the sample holder and the bottom of the sample furnace influenced the $\overline{q}$'s absolute value. The purpose of the present experiment is, however, not the determination of the absolute value of the MF's specific heat but the relative change of $\overline{q}$

as a function of temperature, especially whether or not the peak existed. The MF's mass uncertainty did not influence the determination of the latter properties. We multiply $\overline{q}$ with zero field by suitable constants for samples A_1 and C_1, respectively, so that the individual $\overline{q}$ be equal to those of A_2 and C_2, respectively, at the maximum temperature. Broken lines in Figs. 3(a) and 3(c) denote the renormalized $\overline{q}$ with zero field. The common feature in Figs. 3(a)–3(c) is that the inclination of $\overline{q}$ as a function of T under a field is greater than that with zero field. We discuss this in Sec. IV B.

IV. DISCUSSION

A. MF's heat capacity without taking cluster formation into account

MF's heat capacity $C(T,H)$ under the magnetic field H is expressed by

$$C(T,H)=\left(\frac{\partial U}{\partial T}\right)_H-\mu_o H\left(\frac{\partial M}{\partial T}\right)_H, \tag{16}$$

where U and M are MF's internal energy and magnetization, respectively. In this paper we denote the MF's specific heat and heat capacity as c and C, respectively. If the colloidal particles in the MF do not make clusters, i.e., if they are in a monodispersed state, M is expressed by [30]

$$M(H)=M_s\phi\int_0^\infty f_{\rm dis}(v)L\left(\frac{\mu_o M_s v H}{k_B T}\right)dv, \tag{17}$$

where M_s is the saturation magnetization of the colloidal particles, v is the colloidal particles volume, $f_{\rm dis}(v)$ is a normalized distribution function of the colloidal particles with respect to the particle's volume v, k_B is the Boltzmann constant, and $L(x)$ is the Langevin function defined by

$$L(x)=\coth x-\frac{1}{x}. \tag{18}$$

In the temperature range of the present experiment, M_s can be considered as constant to a good approximation. Accordingly, the magnetic fluid's magnetization M is a function of H/T. In such a case, the internal energy U is independent of M leading $U=U(T)$ [31]. It follows that Eq. (16) is expressed by

$$C(T,H)=C(T,0)-\mu_o H\left(\frac{\partial M}{\partial T}\right)_H. \tag{19}$$

Here, $C(T,0)=dU(T)/dT$ is the MF's heat capacity with zero field.

On the other hand, the typical value of the MF's $(\partial M/\partial T)_H$ is -2×10^{-2} kA/(K m) in order of magnitude [32]. Assume that H is 80 kA/m, the second term on the right-hand side of Eq. (19) is 2 J/(m^3 K) in order of magnitude, which is negligible to the MF's typical heat capacity 1×10^6 J/(m^3 K). In conclusion, if the MF is in a monodispersed phase, the magnetic effect to the MF's heat capacity is negligible within the precision of the present experiment.

B. MF's heat capacity taking cluster formation into account

1. Rough estimation

Let us estimate the mixing entropy $\Delta S_{\rm mix}$ and the mixing enthalpy $\Delta H_{\rm mix}$ of the ordinary MF. Let the solvent be water, the colloidal volume fraction ϕ be 0.1, and, for convenience, all the colloidal particles be spheres of the same radius 5 nm. In such a case, the number of colloidal particles per m^3, n_c, is 1.9×10^{23} m^{-3} and the number of solvent molecules per m^3, n_s, is 3.0×10^{28} m^{-3}. The mixing entropy $\Delta S_{\rm mix}$ is expressed by

$$\Delta S_{\rm mix}=k_B\ln\left[\frac{(n_c+n_s)!}{n_c!n_s!}\right]\approx k_B n_c\left[1-\ln\frac{n_c}{n_s}\right], \tag{20}$$

where $n_c\ll n_s$, was used. Accordingly, $\Delta S_{\rm mix}$ is estimated to be 34 J/(K m^3). If we assume a temperature of $T=300$ K, a mixing enthalpy $\Delta H_{\rm mix}=T\Delta S_{\rm mix}$ is estimated to be 10^4 J/m^3. Comparing the lower limit of the experimental precision, 30 J/kg, it is the same in order of magnitude. (The MF's specific gravity is 10^3 kg/m^3 in order of magnitude.) In addition, the real enthalpy change accompanying the phase transition, ΔH, is expressed by

$$\Delta H=\Delta H_{\rm int}+T\Delta S_{\rm mix}, \tag{21}$$

where $\Delta H_{\rm int}$ is the interaction energy by mixing. As $\Delta H_{\rm int}$ is usually much larger than $T\Delta S_{\rm mix}$, ΔH should be detectable with the present experiment if the phase transition is really of first order.

2. Heat capacity estimation from the Landau formalism

From Eq. (6) we obtain a heat capacity $C(T,H)$ of the MF with agglomerate state as

$$\begin{aligned}C(T,H)=T\left(\frac{\partial^2 G}{\partial T^2}\right)_H&=T\left(\frac{\partial^2 G_o}{\partial T^2}\right)_H+\frac{a\Delta}{T_a}\frac{\partial\Delta}{\partial T}\\&+\left[\frac{a\Delta}{T_a}+a\left(\frac{T}{T_a}-1+f(H)\right)\frac{\partial\Delta}{\partial T}\right]\frac{\partial\Delta}{\partial T}\\&+\left[-\gamma f(H)+a\left(\frac{T}{T_a}-1+f(H)\right)\Delta\right]\frac{\partial^2\Delta}{\partial T^2}.\end{aligned} \tag{22}$$

From Eq. (9)

$$\frac{\partial\Delta}{\partial T}=-\frac{\gamma f(H)}{aT_a^2}\frac{1}{\left(\frac{T}{T_a}-1+f(H)\right)^2} \tag{23}$$

is obtained. Inserting Eqs. (9) and (23) into formula (22), we obtain

$$C(T,H)=C(T,0)-\frac{\gamma^2 f^2(H)}{aT_a^2}\frac{T}{\left(\frac{T}{T_a}-1+f(H)\right)^3}, \tag{24}$$

where $C(T,0)$ is expressed by

$$C(T,0) \equiv T\left(\frac{d^2G_o}{dT^2}\right) \tag{25}$$

or the heat capacity of the magnetic fluid with zero field.

We cannot say anything of significance with respect to the absolute value of the heat capacity due to the experimental error. However, we can say something of significance with respect to the temperature dependence of the heat capacity. Accordingly, let us discuss the temperature dependence of the heat capacity. Differentiating the heat capacity $C(T,H)$ with respect to T, we obtain

$$\frac{\partial C(T,H)}{\partial T} = \frac{dC(T,0)}{dT} + \frac{\gamma^2 f^2(H)}{aT_a^2} \frac{\left(\frac{2T}{T_a}+1-f(H)\right)}{\left(\frac{T}{T_a}-1+f(H)\right)^4}. \tag{26}$$

As the values T_a and f for the present MF are 170 K and 0.1, respectively, in order of magnitude [17], the second term on the right-hand side of Eq. (26) is always positive in the present experimental temperature region. It is consistent with the experimental results of all the six samples, i.e., the heat capacity increase rate with temperature under the field is always greater than those with zero field.

V. CONCLUSION

In our past study, it was found that the strong magneto-optical effect of MF under a magnetic field is due to the phase transition from colloidal particles' monodispersed phase to a phase in which the colloid particles coagulate to anisotropic microclusters. Also, it was found that the temperature dependence of the magnetic birefringence obeys a generalized Curie-Weiss law, which shows that the phase transition is of second order. The order parameter is the ratio of the agglomerated colloidal particles over all the particles. It, however, involved controversy. The monodispersed phase and the anisotropically agglomerated phase belong to different space groups, respectively, and such a transition should be of first order according to the Landau criterion. On the other hand, if fluctuation is taken into account, the transition can be of second order after the Alexander and Amit theory. In the present study, in order to clarify the transition nature, we performed a differential scanning calorimetry experiment on the magnetic fluids to examine an existence of its phase transition heat and to determine whether or not this transition is of first order or second order. We used three different magnetic fluids. The first one is the magnetic fluid of an easy cluster formation, i.e., in it large clusters were observed by an optical microscope under a weak magnetic field. The second one was hard to find the clusters and the third one is the medium between the former two with respect to the cluster formation. We performed DSC measurement on these three samples in the temperature range from 22 to 150 °C with zero magnetic field and with the field of ≈10 kA/m applied by a permanent magnet, respectively. No phase transition heat was observed within an experimental error of 0.03 kJ/kg for all the samples whether or not the field was applied. Accordingly, the present phase transition is concluded to be of second order. The specific heat's increase rate with respect to the temperature under the magnetic field was larger than those with zero field for all the three magnetic fluids. It agrees with the result of the second-order transition theory which was derived from the generalized Curie-Weiss law.

[1] R. E. Rosenweig, *Ferrohydrodynamics* (Cambridge University Press, Cambridge, 1985).

[2] S. Taketomi and S. Chikazumi, *Magnetic Fluids-Principle and Application* (Nokkan Kogyo Schinbun, Tokyo, 1998) [Russian version (Mir, Moscow, 1994)].

[3] P. A. Martinet, Rheol. Acta **13**, 260 (1974).

[4] D. Y. Chung and W. E. Isler, Phys. Lett. **61A**, 373 (1977).

[5] S. Taketomi, Phys. Rev. E **57**, 3073 (1998), **58**, 1175 (1998).

[6] C. F. Hayes, J. Colloid Interface Sci. **52**, 239 (1975).

[7] R. E. Rosensweig and J. Popplewell, Int. J. Appl. Electromagn. Mater. **2**, Suppl. 83 (1992).

[8] J. Cernak, P. Macko, and M. Kasparkova, J. Phys. D **24**, 1609 (1991); J. Cernak and P. Macko, J. Magn. Magn. Mater. **123**, 107 (1993).

[9] Chin-Yih Hong, Herng-Er Horng, F. C. Kuo, S. Y. Yang, H. C. Yang, and J. M. Wu, Appl. Phys. Lett. **75**, 2196 (1999).

[10] L. N. Donselaar, P. M. Frederik, P. Bomans, P. A. Buining, B. M. Humbel, and A. P. Philipse, J. Magn. Magn. Mater. **201**, 58 (1999).

[11] S. Taketomi, N. Inaba, H. Takahashi, and H. Miyajima, J. Phys. Soc. Jpn. Lett. **59**, 3077 (1990).

[12] A. F. Bakuzis, M. F. Da Silva, P. C. Morais, L. S. F. Olavo, and K. Skeff Neto, J. Appl. Phys. **87**, 2497 (2000).

[13] S. Taketomi and R. D. Shull, J. Appl. Phys. **91**, 8546 (2002).

[14] S. Taketomi, M. Ukita, M. Mizukami, H. Miyajima, and S. Chikazumi, J. Phys. Soc. Jpn. **56**, 3362 (1987).

[15] S. Taketomi, M. Ukita, M. Mizukami, H. Miyajima, and S. Chikazumi, J. Magn. Soc. Jpn. **11**, Suppl. S1, 409 (1987).

[16] S. Taketomi, S. Ogawa, H. Miyajima, and S. Chikazumi, IEEE Transl. J. Magn. Jpn. **4**, 384 (1989).

[17] S. Taketomi, H. Takahashi, N. Inaba, H. Miyajima, and S. Chikazumi, J. Phys. Soc. Jpn. **59**, 2500 (1990).

[18] H. Abu-Safia, I. Abu-Aljarayesh, S. Mahmood, and N. A. Yusuf, J. Magn. Magn. Mater. **87**, 333 (1990).

[19] H. Abu-Safia, I. Abu-Aljarayesh, H. M. El-ghanem, and N. A. Yusuf, J. Magn. Magn. Mater. **103**, 19 (1992).

[20] H. W. Davies and J. P. Llewellyn, J. Phys. D **12**, 311 (1979).

[21] L. Sakhnini and J. Popplewell, J. Magn. Magn. Mater. **122**, 142 (1993).

[22] O. Majorana, Phys. Z. **4**, 145 (1902).

[23] J. Shobaki, D. Manasreh, N. A. Yusuf, and I. Abu-Aljarayesh, IEEE Trans. Magn. **32**, 5245 (1996).

[24] L. D. Landau and E. M. Lifshitz, *Statistical Physics* (Pergamon Press, Oxford, 1958), Chap. 14.

[25] P. G. de Gennes, *The Physics of Liquid Crystals* (Oxford University Press, London, 1974), Chap. 2.
[26] S. Alexander and D. J. Amit, J. Phys. A **8**, 1988 (1975).
[27] Y. Saitou, *Principle of Thermal Analysis* (Kyoritsu Shuppan, Tokyo, 1990) (in Japanese).
[28] Y. Saitou, *Principle of Thermal Analysis* (in Ref. [27]), Chap. 3.4.
[29] S. Taketomi, H. Takahashi, N. Inaba, and H. Miyajima, J. Phys. Soc. Jpn. **60**, 1689 (1991).
[30] S. Taketomi and S. Chikazumi, *Magnetic Fluids-Principle and Application* (in Ref. [2]), Chap. 7; R. W. Chantrell, J. Popplewell, and S. W. Charles, IEEE Trans. Magn. **MAG-14**, 975 (1978).
[31] *College Level Exercise in Thermodynamics and Statistical Mechanics*, edited by R. Kubo (Shokabo Publisher, Tokyo, 1961), Chap. 2, Problem 27.
[32] J. Shimoiizaka, K. Nakatsuka, Y. Yoshida, and T. Yamauchi, J. Jpn. Soc. Powder Powder Metall. **24**(4), 118 (1977) (in Japanese).